Distinct High-T Transitions in Underdoped $Ba_{1-x}K_xFe_2As_2$

R. R. Urbano,[1] E. L. Green,[1] W. G. Moulton,[1] A. P. Reyes,[1] P. L. Kuhns,[1] E. M. Bittar,[2] C. Adriano,[2] T. M. Garitezi,[2] L. Bufaiçal,[2] and P. G. Pagliuso[2]

[1]*National High Magnetic Field Laboratory, Florida State University, Tallahassee, Florida 32306-4005, USA*
[2]*Instituto de Física "Gleb Wataghin," Unicamp, 13083-970, Campinas-São Paulo, Brazil*

(Received 19 May 2010; published 31 August 2010)

In contrast with the *simultaneous* structural and magnetic first order phase transition T_0 previously reported, our detailed investigation on an underdoped $Ba_{0.84}K_{0.16}Fe_2As_2$ single crystal unambiguously revealed that the transitions are not concomitant. The tetragonal (τ: $I4/mmm$)-orthorhombic (ϑ: $Fmmm$) structural transition occurs at $T_S \simeq 110$ K, followed by an adjacent long-range antiferromagnetic (AFM) transition at $T_N \simeq 102$ K. Hysteresis and coexistence of the τ and ϑ phases over a finite temperature range observed by NMR experiments confirm the first order character of the τ-ϑ transition and provide evidence that both T_S and T_N are strongly correlated. Our data also show that superconductivity develops in the ϑ phase below $T_c = 20$ K and coexists with AFM. This new observation, $T_S \neq T_N$, firmly establishes another similarity between the hole-doped $BaFe_2As_2$ and the electron-doped iron-arsenide superconductors.

DOI: 10.1103/PhysRevLett.105.107001 PACS numbers: 74.70.Xa, 74.62.−c, 75.50.Ee

The novel class of iron-based high-T_c superconductors LnOM*Pn* (Ln: Lanthanides; M: Mn, Fe, Co, and Ni; *Pn*: P and As) has been one of the most highly investigated superconducting materials since their discovery [1,2]. Their appearance has revitalized the field of superconductivity (SC), providing another window for exploring the interplay between magnetism and unconventional SC. These superconductors are characterized by AFM correlations and long-range ordering throughout the phase diagram, often coexisting with SC deep into the superconducting dome [3–7]. The parent undoped compound usually becomes superconducting upon either chemical (electron or hole) doping or hydrostatic pressure. As a consequence, a dramatic suppression of the AFM order is commonly observed. The K-doped $BaFe_2As_2$ (Ba-122) is the first reported oxygen-free iron-arsenide superconductor with T_c as high as 38 K for the optimal doping $x_K \simeq 0.4$ [8]. Their $ThCr_2Si_2$-type crystal structure possesses a Fe-As layer similar to that of the $LnFeAs(O_{1-x}F_x)$ [1] but not suffering from synthesis issues associated with the control of oxygen or fluorine.

$BaFe_2As_2$ is reported to undergo a simultaneous structural ($\tau - \vartheta$) and AFM transition at $T_0 \simeq 138$ K [8–12]. Neutron diffraction measurements in the ordered state revealed an ordered moment of $0.87\mu_B$ at the Fe site with an ordering wave vector $\mathbf{q} = (1, 0, 1)$ [9], later confirmed to be a commensurate AFM state by zero-field ^{75}As NMR experiments [13]. Coexistence between itinerant AFM and SC has been reported for a wide range of potassium doping, $0.1 \lesssim x_K \lesssim 0.3$ [10,14], and is a common feature in other iron-arsenide compounds [6,11,15,16]. However, until now, the reports regarding the structural or magnetic transition in the Ba-122 family show a conflicting behavior: when $BaFe_2As_2$ is doped with electrons via "in-plane" Co or Ni substitution of Fe ions, the temperature of the first order $\tau - \vartheta$ transition and the AFM ordered phase is monotonically suppressed and the transition separates into two, with the $\tau - \vartheta$ transition occurring at $T_S > T_N$, similar to what is found for LnOM*Pn* compounds [6,15–18]. However, the separation of the structural and AFM transitions has not been observed for the hole-doping case via "out of plane" K substitution of Ba, and, to the best of our knowledge, no experimental evidence of $T_S \neq T_N$ has been reported, even though they present similar phase diagrams [10,14]. Since the AFM state is strongly coupled to the lattice distortions generated by the $\tau - \vartheta$ transition, further investigation is needed to resolve this issue and unravel the interplay between lattice and spin degrees of freedom. NMR is a suitable microscopic technique which can shed new light on the transitions, complementing the bulk measurements. In this Letter we address the problem using a single crystal of underdoped $Ba_{0.84}K_{0.16}Fe_2As_2$. We demonstrate for the first time that $T_S \neq T_N$ for the hole-doped $Ba_{1-x}K_xFe_2As_2$ and suggest that the electronic and magnetic properties of this material share remarkable similarities with the electron-doped iron-arsenides such as $Ba(Fe_{1-x}M_x)_2As_2$ (M = Co, Ni).

Single crystals of $Ba_{1-x}K_xFe_2As_2$ were grown using the Sn-flux method. The previously reported Sn-flux growth method [19] was modified as described in Ref. [20]. The data reported here suggest that our growth method leads to higher quality crystals with very small or negligible Sn contamination. Powder x-ray diffraction on the ground crystals shows single phase with no trace of FeAs impurities as seen in polycrystalline samples. The dc susceptibility measurements $\chi_{dc}(T, H)$ were performed in a Quantum Design Physical Property Measurement System (PPMS) vibrating sample magnetometer with zero-field-cooled (ZFC) and field cooled (FC) procedures with

$H \perp c = 20$ Oe. In-plane electrical resistivity $\rho_{el}(T)$ was measured in a PPMS using the standard four-probe method with $H \perp i_{ab}$. The specific heat $C_p(T)$ measurements were performed on a PPMS with the thermometer and addenda properly calibrated in field. The same crystal used in the bulk measurements was mounted on a NMR probe equipped with a goniometer, which allowed a fine alignment of the crystallographic axes with the external field. The field-swept ^{75}As NMR spectra ($I = 3/2$; $\gamma/2\pi = 7.2919$ MHz/T) were obtained by stepwise summing the Fourier transform of the spin-echo signal.

The T dependence of the in-plane $\rho_{el}(T)$ of our $Ba_{0.84}K_{0.16}Fe_2As_2$ single crystal is shown in Fig. 1. We observe a pronounced anomaly around $T_0 \simeq 105$ K, where $\rho_{el}(T)$ changes its *concavity*, not observed to be as prominent as in the underdoped material [8,21–23]. As shown in the inset of Fig. 1, $d\rho(T)/dT$ demonstrates that the $\tau - \vartheta$ structural phase transition occurs at $T_S \simeq 110$ K, followed by a long-range AFM transition at $T_N \simeq 102$ K. The residual resistivity ratio RRR $\equiv \rho(300\text{ K})/\rho(20\text{ K}) \simeq 7.8$ and the extrapolated residual resistivity $\rho_0 = (287.9 \pm 0.3)\ \mu\Omega$ cm are in good agreement with the self-flux grown K-doped $BaFe_2As_2$ [8,21–23]. These features demonstrate that the Sn-flux technique can yield iron-arsenide samples with high quality. Previous reports have stated that the Sn impurities suppress the AFM ordering temperature by nearly 40%, increases resistivity with decreasing the temperature below T_N, broadens the transition, and alters the critical dynamics [24]. On the other hand, the $\rho(T)$ of our sample does not follow this behavior and continuously decreases with decreasing temperature as shown in Fig. 1.

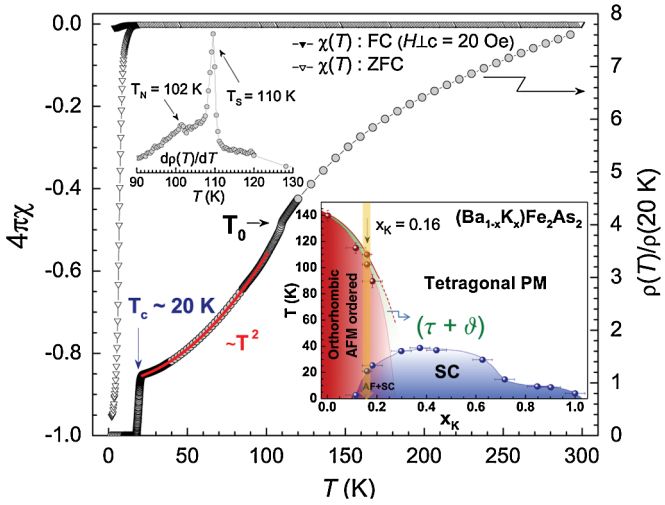

FIG. 1 (color online). T dependence of $\rho_{el}(T)$ for $Ba_{0.84}K_{0.16}Fe_2As_2$. The solid line is a fit of $\rho(T) = \rho_0 + AT^2$ with $\rho_0 = (287.9 \pm 0.3)\ \mu\Omega$ cm and $A = (66.4 \pm 0.1)\ n\Omega$ cm. Top inset: $d\rho(T)/dT$ revealing that $T_S \neq T_N$. The FC and ZFC measurements of $\chi_{dc}(T)$ with $H \perp c = 20$ Oe for the same crystal are also shown. Bottom inset: Phase diagram of $Ba_{1-x}K_xFe_2As_2$ adapted from [14]. The novel coexisting phase $(\tau + \vartheta)$ is highlighted in green. The arrow indicates our sample in the phase diagram.

Further, the observation of $T_S \neq T_N$ cannot be attributed to nonuniform doping distribution given the single and sharp $T_c \simeq 20$ K ($\Delta T_c \lesssim 1.5$ K). It is also a strong evidence that our sample shows negligible or no Sn incorporation.

The magnetic susceptibility measured on the same single crystal is also presented in Fig. 1. FC ($H \perp c = 20$ Oe) and ZFC cycles are shown as a function of temperature. The ZFC χ_{dc} datum shows SC onset at $T_c \simeq 20$ K and a diamagnetic response corresponding to nearly 98% of superconducting volume. The FC curves reveal a much smaller diamagnetic response commonly observed for the underdoped Ba-122. The *anomalies* in $\rho_{el}(T)$ data around T_0 are only observed in χ_{dc} with fields $H \gtrsim 1$ T (not shown), with temperature dependence similar to that observed for $BaFe_2As_2$ [25].

In Fig. 2 we show the T dependence of the specific heat C_p/T plotted as a function of temperature for $H = 0$ and 9 T for the same single crystal. C_p/T is essentially field independent except near T_S and T_N, which indicates that the magnetic field might have some influence over the conservation of the entropies associated with each transition.

In contrast with the single anomaly observed previously in the C_p of K-doped Ba-122 samples [21], we observe two distinct peaks occurring at slightly different temperatures consistent with $d\rho(T)/dT$. We associate the sharper peak at $T_S \simeq 110$ K with the first order $\tau - \vartheta$ transition and the broader one at $T_N \simeq 102$ K as the AFM transition. This new observation for the underdoped $Ba_{1-x}K_xFe_2As_2$ is consistent with the double transitions observed in electron-doped Ba-122 [15,16,18]. It has been suggested that the splitting is due to either the formation of fluctuating AFM domains below T_S, which become pinned at lower T_N, or an Ising transition at T_S followed by AFM order at T_N [26,27]. Both scenarios involve coupling

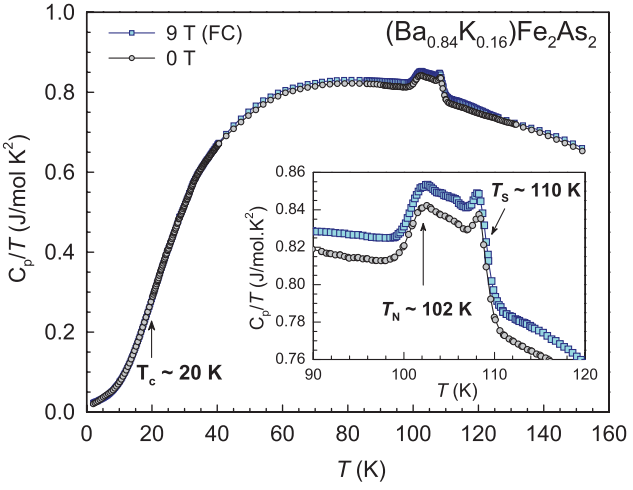

FIG. 2 (color). T dependence of C_p/T for $Ba_{0.84}K_{0.16}Fe_2As_2$. Inset: A blowup of the T_S and T_N transitions. Arrows indicate the onset of the $\tau - \vartheta$ transition at $T_S \simeq 110$ K and the long-range AFM order at $T_N \simeq 102$ K.

between lattice and magnetic fluctuations [28]. C_p/T shows no visible anomaly at $T_c \simeq 20$ K where bulk SC is evident and inferred from Fig. 1. This behavior agrees with a previous report on the underdoped $Ba_{1-x}K_xFe_2As_2$ with $x = 0.1$ and 0.2 [21]. However, we were able to identify the maximum of a broad bump around 20 K from the derivative $dC_p(T)/dT$ (not shown). The peak defining T_c in the C_p data is only evident for optimally doped samples ($x_K \simeq 0.4$) when long-range AFM order is fully suppressed [21]. We also point out that the transition temperatures observed by χ_{dc}, $\rho_{el}(T)$, and C_p/T data are consistent with the phase diagram with $x_K = 0.16$ (Fig. 1).

Motivated by the possible coupling between the AFM order and the structural distortion we have also performed a microscopic investigation by NMR experiments. Figure 3(a) presents the ^{75}As-NMR spectra obtained by sweeping up $H \perp c$ at constant frequency $\nu = 62.238$ MHz. The spectra present the typical features of a nuclear spin $I = 3/2$ with Zeeman and quadrupolar couplings. The spectra at 120 K represent the normal paramagnetic (PM) state while the broad spectra at 4.2 K belong to the coexisting AFM + SC states.

In the PM state, the spectra show a sharp central line with a FWHM of 36 kHz (~50 Oe) and two sets of broader satellite lines split by the quadrupolar interaction of the As nuclei with the local electric field gradient (EFG). The single and sharp central transition is a microscopic evidence for a homogeneous sample. The satellites are split due to the strain introduced by doping, the different

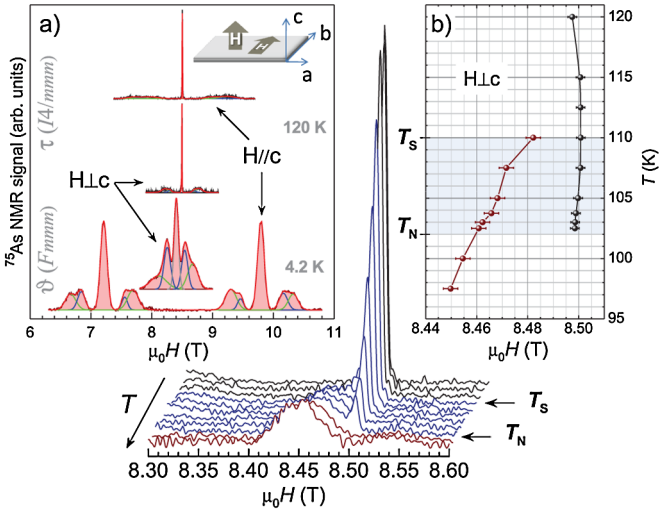

FIG. 3 (color online). (a) ^{75}As NMR spectra of $Ba_{0.84}K_{0.16}Fe_2As_2$ at 120 K (PM state) and 4.2 K (AFM + SC coexisting state) for $H \parallel c$ and $H \perp c$. In the PM state, the spectra show a sharp central transition ($+1/2 \leftrightarrow -1/2$) at 8.5 T with broad satellite peaks from the ($\pm 1/2 \leftrightarrow \pm 3/2$) transitions. Below T_N, the $H_{int} \parallel c$ symmetrically splits the NMR spectra for $H \parallel c$. For $H \perp c$, only a shift is observed [12]. The main panel presents the central transition with $H \perp c$ where τ-ϑ phase coexistence is evident. (b) Peak position of the lines obtained from Gaussian fits.

number of Ba neighbors to As sites, and the broadening is due to a distribution of both EFG and hyperfine fields. The quadrupole splitting is proportional to the EFG at the As, V_{zz}, through the relation $\nu_Q = eQV_{zz}/2\sqrt{1+\eta^2/3}$, where Q is the nuclear quadrupole moment of ^{75}As and η is the asymmetry parameter of the EFG ($\eta = 0$ for the τ phase). V_{zz} arises from the hybridization between the As-4p and the Fe-3d orbitals with an added contribution from any noncubic distribution of surrounding ions, resulting in two distinct sets of quadrupole satellite lines through doping (due to different number of K neighbors) with different quadrupole frequencies, $\nu_Q = 4.07(1)$ and 2.94(1) MHz. These are larger than $\nu_Q = 2.21$ MHz observed in the undoped system [12] and agree with previous observations that ν_Q increases with increased doping [29,30]. It also confirms that this sample has electronic but not chemically (or macroscopically) segregated inhomogeneities [5]. The twinned structural domains are only observed in the orthorhombic (ϑ) ordered phase [12] and may be responsible for the line broadening below T_N.

Below the AFM ordering temperature, internal hyperfine fields H_{int} develop along the c axis generated by the commensurate AFM ordered Fe moments at the As. These H_{int} split the ^{75}As-NMR spectra, doubling the number of resonance lines when $H \parallel c$ [Fig. 3(a)]. The lines broaden due to a distribution of EFG and static hyperfine fields produced by lattice distortions at the $\tau - \vartheta$ transition. The internal field $H_{int}^{\parallel c}(4.2\text{ K}) \simeq 1.29(1)$ T is obtained from the splitting of the central lines (after taking the second order quadrupolar shift ν_Q^2/ν_0 and the demagnetization contribution into account), since the resonance field is given by $H_{eff} = H_0 \pm H_{int}$. This agrees with the only NMR report so far in the underdoped regime, $H_{int} = 1.23(5)$ T on a $x = 0.3$ aligned powder sample taken at zero field [31]. However, these values are smaller than $H_{int} \simeq 1.48(2)$ T for $BaFe_2As_2$ [12,30,31]. It has been suggested that the H_{int} decreases with increasing K concentration [31]. Since H_{int} is a direct measure of the magnetic order parameter, this result is consistent with the suppression of T_N and the emergence of SC upon increasing K doping (see phase diagram in Fig. 1).

Since $H_{int} \parallel c$, when $H \perp c$, the resonance field is given by the magnitude of the vector sum of the mutually orthogonal external and internal fields, $H_{eff} = \sqrt{H^2 + H_{int}^2}$, causing the shift of the unsplit ^{75}As-NMR spectra towards lower fields as displayed in Fig. 3(a) [12]. The main panel of Fig. 3 shows the central transition of the ^{75}As-NMR spectra with $H \perp c$ at several temperatures above and below $T_S \simeq 110$ K and $T_N \simeq 102$ K. Figure 3(b) presents the peak position of the lines obtained from Gaussian fits. The single narrow central transition for temperatures $T \geq T_S$ represents the τ phase in the PM state. The spectra for $T \lesssim T_S$ reveal a sudden appearance of a broad line at lower fields coexisting with the narrow line for a finite T range. The broad peak grows rapidly, while the sharp peak is

suppressed with decreasing temperature. Also the peak intensity of the spectrum revealed hysteresis around T_S. We define this temperature as the onset of the first order structural transition $\tau - \vartheta$. The coexistence of both τ and ϑ phases reflects the fact that the $\tau - \vartheta$ and AFM transitions are intimately related. We propose that the transition takes place by the growth of the ϑ domains nucleating inside the τ phase. It requires greater undercooling to further develop the nucleation sites into the bulk, and the coexisting phases remain over a relatively wide range of temperature. Long-range AFM is not fully developed until the percolation limit between the ϑ phases is achieved, and it is only observed when the structure is entirely orthorhombic with minor or no remnant τ phase. We thus define the temperature where this happens as $T_N = 102$ K, in agreement with the bulk measurements (Figs. 1 and 2). The shift of the broad peak also changes its behavior dramatically around T_N and, below that, it follows the T dependence of the magnetic order parameter $M(T) = M_0[1 - (T/T_N)]^{\alpha}$ as a consequence of the ordered Fe moments generating the $H_{\mathrm{int}}^{\|c}$ at the ^{75}As nuclei. This picture could be a consequence of the stress and/or pressure at the boundaries of the twinned domains due to the orthorhombic distortion and thus lowering T_N [28]. Such an effect could lead to a nonmonotonic behavior of the order parameter but with a monotonic variation in temperature as suggested by a recent neutron scattering study on the related $SrFe_2As_2$ compound [32]. Li and co-workers claim that the structural transition is probably an order-disorder one, based on the fact that they observed some residual τ phase below the transition T_S and some ϑ above it [32]. Similar behavior is also found in $Ba(Fe_{0.953}Co_{0.047})_2As_2$ [6]. In contrast to this observation, the NMR data in Fig. 3 reveal a complete disappearance of the sharp peak associated with the τ phase below $T_N \simeq 102$ K and show no traces of the broad peak associated with the twinned ϑ-ordered phase above $T_S \simeq 110$ K, attesting that the remnant minor structural phases are absent or negligible in our sample. Similar behavior in agreement with our results has been recently observed by an imaging technique in $SrFe_2As_2$ [33].

Regarding the coexistence of the orthorhombic AFM phase with SC suggested by the bulk measurements, we conclude from our NMR investigation that they coexist microscopically in underdoped compositions, at least on a lattice parameter length scale as inferred from the spin-spin and spin-lattice relaxation rates, $1/T_2$ and $1/T_1$, respectively (not shown). In addition, we notice little or no change in the ^{75}As NMR spectra while crossing T_c and we observe the broad spectra associated with the ϑ structure within the SC phase, with no traces of the τ phase, confirming the crystallographic homogeneity of the sample. This clearly indicates that the ^{75}As NMR signal is predominantly from the AFM regions even below the SC transition. Since the H_{int} is a direct measure of the magnetic order parameter, its suppression by roughly 15% suggests that the ordered Fe moment must be decreasing with addition of potassium and provides evidence that the AFM order might be related with the SC. The results reported here demonstrate that coupling to the lattice plays an important role in the AFM transition and may be a remarkable signature within the underdoped region of the phase diagram of the iron-arsenide superconductors.

We thank L. Balicas, N. Curro, and L. P. Gor'kov for relevant discussions. Work at NHMFL was performed under the auspices of the NSF (DMR-0654118) and the State of Florida. Work at Unicamp was supported by Fapesp, CNPq, and Capes.

[1] Y. Kamihara *et al.*, J. Am. Chem. Soc. **130**, 3296 (2008).
[2] X. H. Chen *et al.*, Nature (London) **453**, 761 (2008).
[3] D. S. Inosov *et al.*, Nature Phys. **6**, 178 (2010).
[4] A. J. Drew *et al.*, Nature Mater. **8**, 310 (2009).
[5] J. T. Park *et al.*, Phys. Rev. Lett. **102**, 117006 (2009).
[6] D. K. Pratt *et al.*, Phys. Rev. Lett. **103**, 087001 (2009).
[7] A. D. Christianson *et al.*, Phys. Rev. Lett. **103**, 087002 (2009).
[8] M. Rotter, M. Tegel, and D. Johrendt, Phys. Rev. Lett. **101**, 107006 (2008).
[9] Q. Huang *et al.*, Phys. Rev. Lett. **101**, 257003 (2008).
[10] H. Chen *et al.*, Europhys. Lett. **85**, 17 006 (2009).
[11] N. Ni *et al.*, Phys. Rev. B **78**, 214515 (2008).
[12] K. Kitagawa *et al.*, J. Phys. Soc. Jpn. **77**, 114709 (2008).
[13] H. Fukazawa *et al.*, J. Phys. Soc. Jpn. **77**, 093706 (2008).
[14] M. Rotter *et al.*, Angew. Chem., Int. Ed. **47**, 7949 (2008).
[15] C. Lester *et al.*, Phys. Rev. B **79**, 144523 (2009).
[16] R. Prozorov *et al.*, Phys. Rev. B **80**, 174517 (2009).
[17] M. A. McGuire *et al.*, Phys. Rev. B **78**, 094517 (2008).
[18] J.-H. Chu *et al.*, Phys. Rev. B **79**, 014506 (2009).
[19] N. Ni *et al.*, Phys. Rev. B **78**, 014507 (2008).
[20] Elemental Ba, K, Fe, and As were added to Sn in the ratio of $(Ba/K)Fe_2As_2$:Sn = 1:20 and placed in a 5 ml Al_2O_3 crucible which was covered with quartz wool and sealed in an evacuated quartz ampoule. The ampoule was heated to 850 °C for 0.5 h and cooled at 5 °C per hour down to 500 °C. After 48 h of in-flux annealing at 500 °C, the crystals were separated from the Sn flux in a centrifuge.
[21] M. Rotter *et al.*, New J. Phys. **11**, 025014 (2009).
[22] Z. S. Wang *et al.*, Phys. Rev. B **78**, 140501(R) (2008).
[23] X. G. Luo *et al.*, Phys. Rev. B **80**, 140503(R) (2009).
[24] S. -H. Baek *et al.*, Phys. Rev. B **78**, 212509 (2008).
[25] M. Rotter *et al.*, Phys. Rev. B **78**, 020503(R) (2008).
[26] I. I. Mazin and M. D. Johannes, Nature Phys. **5**, 141 (2009).
[27] Y. Qi and C. Xu, Phys. Rev. B **80**, 094402 (2009).
[28] V. Barzykin and L. P. Gorkov, Phys. Rev. B **79**, 134510 (2009).
[29] M. H. Julien *et al.*, Europhys. Lett. **87**, 37 001 (2009).
[30] H. Mukuda *et al.*, Physica (Amsterdam) **469C**, 559 (2009).
[31] H. Fukazawa *et al.*, J. Phys. Soc. Jpn. **78**, 033704 (2009).
[32] H. Li *et al.*, Phys. Rev. B **80**, 054407 (2009).
[33] J. C. Loudon *et al.*, Phys. Rev. B **81**, 214111 (2010).